Trimerized ground state of the spin-1 Heisenberg antiferromagnet on the kagome lattice

Hitesh J. Changlani[1,2,3] and Andreas M. Läuchli[3]

[1]*Department of Physics, University of Illinois at Urbana-Champaign, Urbana, Illinois 61801, USA*

[2]*Institute for Quantum Optics and Quantum Information of the Austrian Academy of Sciences, A-6020 Innsbruck, Austria*

[3]*Institut für Theoretische Physik, Universität Innsbruck, A-6020 Innsbruck, Austria*

We study the phase diagram of the spin-1 quantum bilinear-biquadratic antiferromagnet on the kagome lattice using exact diagonalization and the density matrix renormalization group algorithm. The SU(3)-symmetric point of this model Hamiltonian is a spontaneously trimerized state whose qualitative nature persists even at the Heisenberg point, a finding that contrasts previous proposals. We report the ground state energy per site of the Heisenberg model to be $-1.410(2)$ and establish the presence of a spin gap.

Introduction. The discovery of experimental realizations of kagome antiferromagnets [1,2] and indications that they have exotic ground states has spurred immense activity in the past few years. The nature of the ground state is unresolved for even the simplest realistic model, the nearest neighbor spin-1/2 kagome Heisenberg antiferromagnet (KHAF) [3–10]. However, recent advances in numerical algorithms have enhanced our understanding of these systems [10–15].

In contrast to the spin $S = 1/2$ case, little has been definitively established for the ground state of the $S > 1/2$ case. When S is large, as is the case for the $S = 5/2$ iron jarosite $KFe_3(OH)_6(SO_4)_2$ [16], long-range magnetic order of the $\sqrt{3} \times \sqrt{3}$ type is expected [17,18]. However, for the intermediate spin case, $S = 1$ [19–21] and $S = 3/2$ [22], the theoretical situation is unclear. There exist several experimental motivations [23] for studying this problem. For example, $KV_3Ge_2O_9$ [24] and $BaNi_3(OH)_2(VO_4)_2$ [25] are candidates for $S = 1$, and chromium jarosite has been reported to be a $S = 3/2$ kagome antiferromagnet [26].

The focus of this Rapid Communication is the $S = 1$ case, with emphasis on the KHAF. Previous numerical studies of the $S = 1$ *XXZ* model with on-site anisotropy [27,28] have shed light on the phase diagram, but the approach is limited for the KHAF. Recent coupled cluster calculations [21] show that the $S = 1$ KHAF has no long-range magnetic order, in contrast to previous analytic results [20]. Thus, the definitive characterization of the ground state remains an open question.

Based on exact diagonalization (ED) of the $S = 1$ KHAF, Hida proposed that the ground state is a hexagonal singlet solid (HSS) with a spin gap [19]. The HSS is a translationally invariant state that is described by an Affleck-Kennedy-Lieb-Tasaki (AKLT) [29] type wave function. As is schematically depicted in Fig. 1(b), all the spin-1's fractionalize into two spin-1/2's and then the spin-1/2's on every hexagon form a singlet state. However, a recent experiment [30] with m-MPYNN · BF_4, believed to be a $S = 1$ KHAF, has observed magnetization plateaus different from those predicted by the HSS phase [31], calling for a review of this picture.

In this Rapid Communication, we use ED and the density matrix renormalization group (DMRG) algorithm [32] for cylindrical geometries [33]. We show that even though the HSS has a competitive energy (≈ -1.36 per site) in comparison to the DMRG results (≈ -1.41 per site), the qualitative picture obtained from the latter is that of a trimerized ground state,

schematically illustrated in Fig. 1(a). This state, referred to as the simplex-solid [34] or simplex-valence bond crystal, is a symmetry-broken state where the three spin-1's living on each up (or equivalently down) pointing triangle form collective singlets or "trimers."

We find no long-range spin-spin correlations and a finite spin gap of ~ 0.2–0.3 for the choice of lattice geometries studied. In addition, the energy of a recently proposed ground state candidate Z_2 spin liquid, the resonating AKLT state (RAL) [35], is found to be higher than both the HSS and the trimerized state found in DMRG.

We have considered the phase diagram of the nearest neighbor bilinear-biquadratic model,

$$\mathcal{H} = J_{bl} \sum_{\langle ij \rangle} \mathbf{S}_i \cdot \mathbf{S}_j + J_{bq} \sum_{\langle ij \rangle} (\mathbf{S}_i \cdot \mathbf{S}_j)^2, \qquad (1)$$

where $\langle ij \rangle$ refer to nearest neighbor pairs, J_{bl} is the bilinear Heisenberg coupling (set to $J_{bl} = 1$), and J_{bq} is the biquadratic coupling. While a previous tensor network study showed the ground state to be a simplex solid at the SU(3)-symmetric point ($J_{bl} = J_{bq}$) [36], here we provide evidence that this trimerization survives on reducing the magnitude of J_{bq} all the way to zero. A quantum phase transition to a ferroquadrupolar spin nematic is observed only at $J_{bq} \sim -0.16$.

The Heisenberg point. We consider $J_{bq} = 0$, the Heisenberg point, and assess the quality of the HSS wave function with respect to ED calculations. Following Hida [19], we associate two spin-1/2 degrees of freedom (labeled by α and β) with every spin-1, and define

$$|+1\rangle \equiv \frac{\psi_{1/2,1/2}}{\sqrt{2}}, \quad |0\rangle \equiv \psi_{1/2,-1/2}, \quad |-1\rangle \equiv \frac{\psi_{-1/2,-1/2}}{\sqrt{2}}, \qquad (2)$$

where $\psi_{\alpha,\beta} \equiv \frac{1}{\sqrt{2}}(\psi_\alpha \otimes \psi_\beta + \psi_\beta \otimes \psi_\alpha)$. $\psi_{\alpha(\beta)}$ is the wave function of a single spin-1/2. Then the HSS wave function is defined to be

$$\Phi_{\text{HSS}} = \bigotimes_i \psi_{\alpha_i,\beta_i} \prod_i \left(\delta_{\alpha,\gamma_i} + \delta_{\beta,\gamma_i} \right) \prod_p w^{\gamma_{i_p},\gamma_{j_p},\gamma_{k_p},\gamma_{l_p},\gamma_{m_p},\gamma_{n_p}}, \qquad (3)$$

where $i_p, j_p, k_p, l_p, m_p, n_p$ refer to the sites on the elementary hexagon (given the label p) and γ_{i_p} through γ_{n_p} are the spin-1/2 state labels ($\pm 1/2$) for those sites. $w^{\gamma_{i_p},\gamma_{j_p},\gamma_{k_p},\gamma_{l_p},\gamma_{m_p},\gamma_{n_p}}$ is the
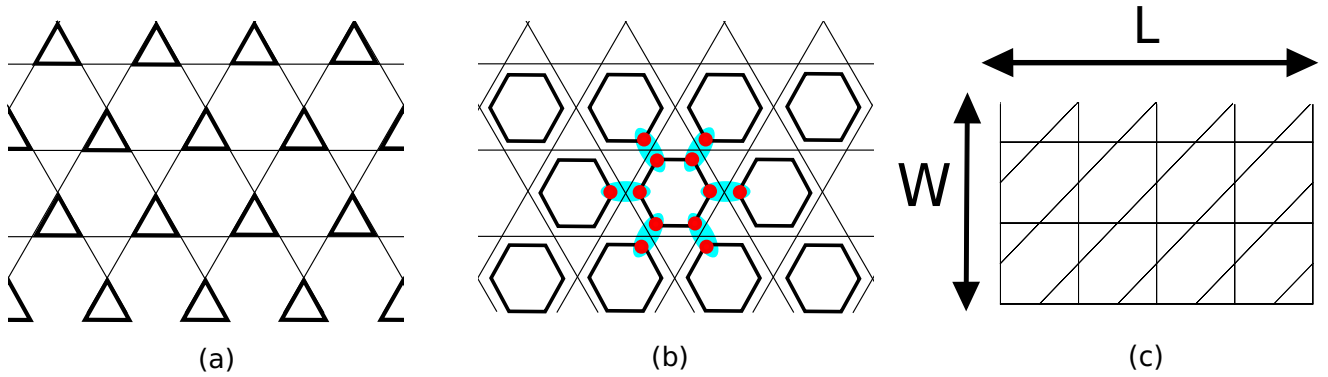
FIG. 1. (Color online) (a) shows a schematic of the simplex solid on the kagome lattice. The bond thicknesses represent the relative magnitude of the bond energy. (b) shows a schematic of the hexagon singlet solid (HSS). Each spin-1 (depicted in blue) fractionalizes into two spin-1/2 (shown by red circles). The spin-1/2's on the hexagons form a singlet, shown by the black lines connecting them. (c) shows the cylindrical geometry used in the DMRG calculation. Periodic boundary conditions in the width direction have not been shown.

coefficient of the lowest-energy singlet state of a $S = 1/2$ nearest neighbor Heisenberg model on a hexagon.

Table I shows the energy of the HSS, the RAL [35], and ground state wave functions from ED for various finite clusters with periodic boundary conditions; the geometries and nomenclature are the same as in Ref. [19]. We estimate the HSS energy in the thermodynamic limit to be −1.36 per site [37]. This is comparable to the energy from ED (roughly −1.4), and much lower than the RAL energy, suggesting that the HSS is a competitive candidate for the ground state.

However, a clear picture of the ground state emerges only for larger systems, which were studied with DMRG. Cylinders with periodic boundaries in the width (W) direction and open boundaries in the length (L) direction, as shown in Fig. 1(c), were chosen for the simulations. In order to have complete hexagons, even widths were considered.

The number of renormalized states (denoted by m) kept in the DMRG simulations were typically 2000, 3000, and 4000 for widths 4, 6, and 8, respectively. On cylinders with widths 4 and 6, and odd lengths (these have equal numbers of up and down pointing triangles), a pattern of alternating strong and weak trimers propagates from both the left and right edges. These competing patterns superpose in the center of the finite sample, leading to uniform bond energies; the bond energy is defined as $\langle \mathbf{S}_i \cdot \mathbf{S}_j \rangle$ for nearest neighbor sites i, j. On the even-length cylinders, which have more down triangles than up, the leftmost row of boundary sites forms dimers, effectively decoupling them from the bulk of the system. Thus,

the even-length cylinders have bulk properties similar to the odd-length cylinders.

For width 8 cylinders, the tendency to form dimers along the width direction is suppressed and a robust trimerization pattern is observed throughout the bulk. For the odd lengths, DMRG tends to break the symmetry between the up and down pointing triangles, which we take to be evidence that the system prefers to trimerize. This is a "finite m" effect, as an *exact* calculation should yield a perfect superposition of both trimer states.

To estimate the energy per bond in the thermodynamic limit, we used two procedures. First, we considered the total energy $E(L,W)$ of the cylindrical sample and fit it to the functional form

$$E(L,W)/N_b(L,W) = e_b + a_1/L + a_2/L^2, \qquad (4)$$

where $N_b(L,W)$ is the number of bonds and e_b, a_1, a_2 are fit parameters. In the second method, we average the bond energies on a central feature, such as the bowtie or "star" consisting of three up and three down triangles. We refer to this estimate as the "bulk" energy. Figure 2(a) shows the length dependence of the energy and its extrapolation to infinite length for different cylinder widths. Both analyses yield similar estimates; For the width 4, 6, and 8 cylinders the values of the energy per bond are −0.7117(1), −0.7067(1), and −0.7058(4), respectively. Assuming small variations for energy estimates beyond $W > 8$, the energy per bond in the thermodynamic limit is −0.705(1), which in terms of the energy per site (E_0) is −1.410(2). This is comparable to (and slightly lower than) the coupled cluster result of $E_0 = -1.4031$ [21,38].

Next, we verified the presence of a spin gap in the thermodynamic limit by calculating the energy difference between the singlet and triplet states for both even- and odd-length cylinders. Our results are shown in Fig. 2(b). The magnetization of the first excited state is distributed over the entire sample, establishing that the excitation is a bulk one. The large variation in the energy gap for the width 4 and the other larger cylinders is a finite size effect; this qualitative difference is also seen in ground state energy estimates. The trends in the spin gap for width 6 and 8 cylinders indicate that its value is in the range 0.2–0.3.

TABLE I. Energy per site for the hexagon singlet state (HSS), resonating AKLT state (RAL), and exact diagonalization (ED) wave functions on kagome clusters of different sizes with periodic boundary conditions.

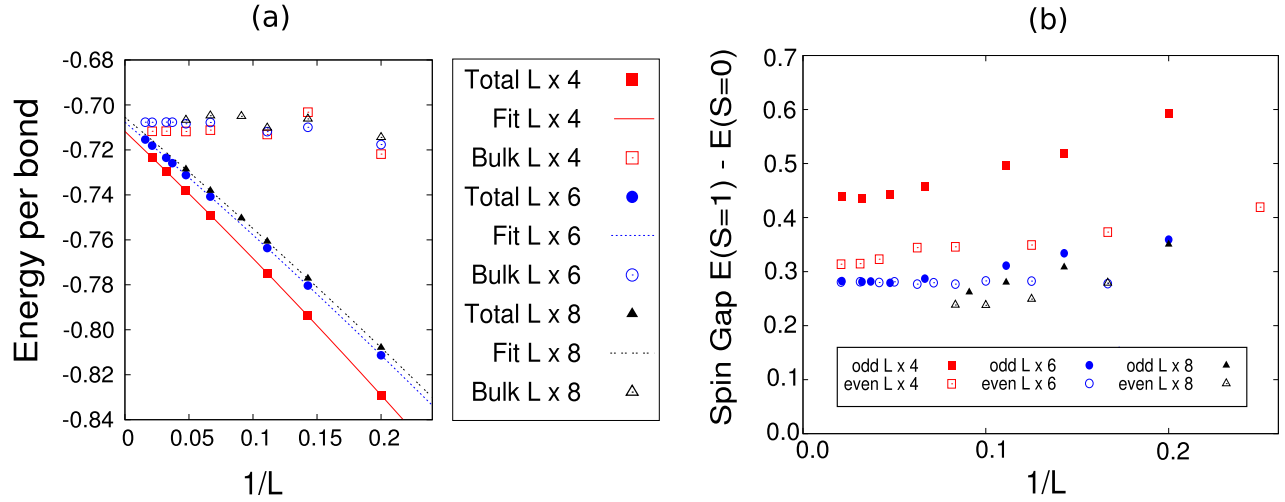| Wave function	Lattice				
	12	15	18a	18b	∞
HSS	−1.38781	−1.36024	−1.36108	−1.36995	≈ −1.36
RAL [35]				−1.38	−1.2696
ED	−1.46841	−1.44958	−1.45110	−1.43926	≈ −1.4

FIG. 2. (Color online) (a) The total ground state energy per bond for cylinders of odd lengths and different widths is extrapolated to infinite length by fitting to the functional form, Eq. (4). The bulk energy (see text) is also shown. (b) shows the spin gap for various cylinder widths and lengths. The estimated gap in the infinite length limit is finite.

To build further confidence in these results, we study the bilinear-biquadratic (BLBQ) model (1) and use J_{bq} as a knob to connect the Heisenberg point to the SU(3) point. Analyzing other Hamiltonians should lead to similar conclusions. For example, an extended Heisenberg model studied by Cai *et al.* [39] also has a trimerized ground state.

The bilinear-biquadratic (BLBQ) model. For insights into the BLBQ model, we performed ED calculations on a 21-site sample with periodic boundary conditions. Multiple low-energy excited state energies, resolved by spatial momenta, have been plotted in Fig. 3. On tuning J_{bq} from 1 towards 0, we find no energy crossings in the first few states in the low-energy

manifold. In the range $-0.2 < J_{bq} < -0.1$, a marked decrease in energy spacings (or increased crowding of energy levels) and the appearance of a small finite size gap are indicative of a quantum phase transition.

Next, we look for signatures of possible phase transitions as a function of J_{bq} by monitoring the wave function fidelity [40], defined as $F \equiv \langle \psi(p)|\psi_{\text{ref}}\rangle$, where $|\psi(p)\rangle$ is a wave function dependent on parameters p and $|\psi_{\text{ref}}\rangle$ is a reference wave function. Figure 4 shows fidelities of the 12- and 21-site clusters as a function of J_{bq}/J_{bl}, by fixing the reference wave function to be the ground state wave function of the SU(3)
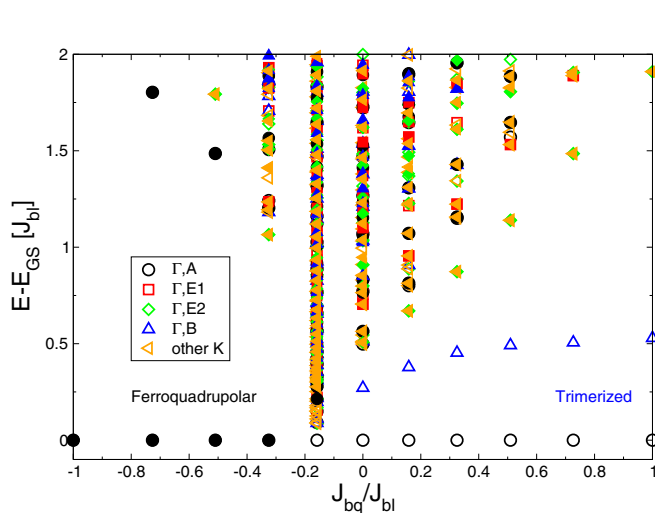

FIG. 3. (Color online) The low-energy spectrum of the BLBQ model on the 21-site kagome lattice, resolved by lattice momenta, as a function of J_{bq}, is shown. On tuning J_{bq} from 1 towards 0, the low-energy features appear adiabatically connected, suggesting the persistence of the trimerized phase to the Heisenberg point. Qualitative changes in the energy spectrum seen at a negative value of J_{bq} indicate a quantum phase transition to a ferroquadrupolar phase.
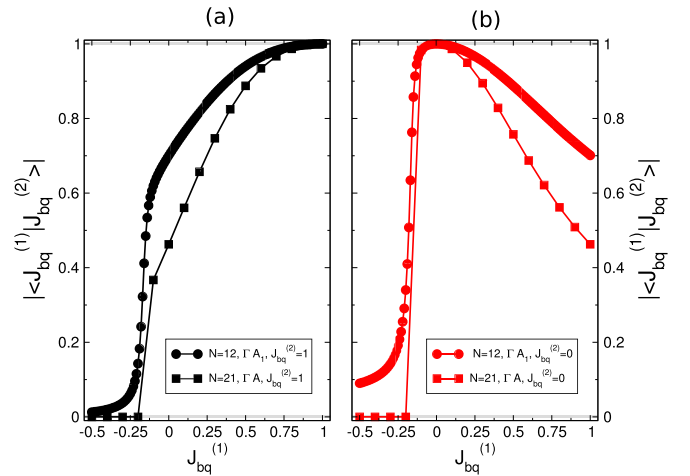
FIG. 4. (Color online) The fidelity of ground state wave functions from ED of 12- and 21-site clusters is shown as a function of J_{bq} for two reference wave functions. The reference wave function is chosen to be the ground state of (a) the SU(3)-symmetric model, known to favor a trimerized (simplex solid) phase, and (b) the Heisenberg model, whose qualitative nature remains to be established and is the subject of this study. An abrupt change in fidelity is found to occur in both cases in the range $-0.2 < J_{bq} < -0.13$.
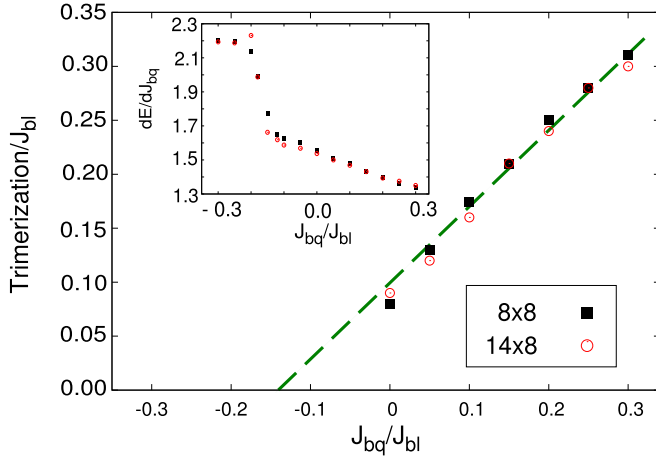
FIG. 5. (Color online) The main panel shows the trimerization order parameter for the 8×8 and 14×8 kagome lattice as a function of J_{bq}. The dashed line gives an extrapolated estimate of the J_{bq}^* at which the trimerization vanishes. Inset: Derivative of the total energy per bond with respect to J_{bq} shows an abrupt change around the same value of $J_{bq}^* \approx -0.16$.

model [Fig. 4(a)] and the Heisenberg model [Fig. 4(b)]. In either case, the fidelity decreases on going away from the chosen reference point and with increasing lattice size; the latter is expected because overlaps involve the multiplication of an increasing number of factors less than 1. We consider an overlap of 0.45 between the Heisenberg and SU(3)-symmetric point wave functions for the 21-site lattice to be large and view the sharp fall in fidelity in the range $-0.2 < J_{bq} < -0.13$ to be the only sign of a phase transition. We thus infer that the Heisenberg point corresponds to a trimerized ground state.

The inferences from ED are verified on larger samples using DMRG, by considering a variety of metrics. First, as shown in the inset of Fig. 5, the energy as a function of J_{bq} has a discontinuity in its derivative at a value $J_{bq} \approx -0.16$. This value coincides with the location of the minimum of the singlet-singlet gap, obtained by taking the energy difference of the lowest $S_z = 0$ states in the DMRG method (not shown in the plot). However, the most direct evidence is that of a nonzero trimerization order parameter, defined to be

$$\text{Trimerization} \equiv |\langle \mathbf{S}_i \cdot \mathbf{S}_j \rangle_\Delta - \langle \mathbf{S}_i \cdot \mathbf{S}_j \rangle_\nabla|, \qquad (5)$$

where $\langle \mathbf{S}_i \cdot \mathbf{S}_j \rangle_{\Delta(\nabla)}$ is the average spin-spin bond correlator on an up (down) pointing triangle. The trimerization is (relatively) uniform throughout the sample on the width 8 cylinders and these data are used to determine the critical J_{bq}^* at which the phase transition occurs. When J_{bq} is close to J_{bq}^*, the trimerization is small and inhomogeneous and the presence of the open boundaries becomes important. This is why we used only the values of trimerization for $J_{bq} \geqslant 0$ and extrapolated them to $J_{bq} < 0$ in Fig. 5.

Below $J_{bq} \lesssim -0.16$, a ferroquadrupolar spin nematic is present, a generic occurrence in many $S = 1$ antiferromagnets with negative biquadratic couplings [41]. This state has $\langle \mathbf{S_i} \rangle =$

0 but still breaks the spin rotational symmetry. This is verified by the observation that $\langle S_i^+ S_i^- \rangle \neq \langle (S_i^z)^2 \rangle$ and that $\langle (S_i^z)^2 \rangle$ abruptly changes from $0.66(=2/3)$ to ≈ 0.4 at the critical point.

Conclusion. We have performed ED and DMRG calculations on the spin-1 kagome antiferromagnet with bilinear and biquadratic terms. We find evidence for trimerization at the Heisenberg point, which is not consistent with the hexagonal singlet state (HSS) picture [19], nor with the $\sqrt{3} \times \sqrt{3}$ order predicted by $1/S$ methods [20]. We also estimated the location of the phase transition from the trimerized state to the spin-nematic phase to be $J_{bq}^* \sim -0.16$.

Recently, Li *et al.* [35] proposed a spin liquid ground state for the $S = 1$ KHAF, the resonating AKLT state (RAL), obtained by creating a uniform superposition of all possible "AKLT loops." On an 18-site lattice, the RAL energy is marginally lower than that of the HSS, but in the infinite lattice limit it is significantly higher [35]. A plausible reason is that the RAL is dominated by long loops that are still relatively short on an 18-site lattice. Presumably, if the longest loops are penalized (i.e., a loop tension is added in the wave function), the RAL energy could improve significantly. Whether such a modification preserves the spin liquid properties or alternately drives it to a confining phase, such as the trimerized phase, is not known. Since the trimerization strength is small, it will be interesting to see if additional interactions at the Heisenberg point stabilize the RAL, HSS, or other exotic states.

Finally, we comment on the possible experimental consequences of our finding. Since trimerization does not change the magnetic unit cell structure of the kagome lattice, we still expect to see the 1/3 magnetization plateau for the $S = 1$ KHAF, based on the Oshikawa-Yamanaka-Affleck criterion [42]. However, prominent magnetization plateaus seen in the experiment with m-MPYNN · BF$_4$, which also has a slight $\sqrt{3} \times \sqrt{3}$ distortion [30], correspond to 1/2 and 3/4. This is indicative of an enlarged magnetic unit cell with 12 atoms. Thus, we intend to understand the effective low-energy Hamiltonian better to resolve this issue.

Note added. Recently, we became aware of two related works. Liu *et al.* [43] independently concluded that the ground state of the $S = 1$ KHAF is a simplex solid, using complementary tensor network methods. Picot *et al.* [44] studied the $S = 1$ KHAF in a magnetic field; their zero field results support the trimerization picture.

[1] J. S. Helton, K. Matan, M. P. Shores, E. A. Nytko, B. M. Bartlett, Y. Yoshida, Y. Takano, A. Suslov, Y. Qiu, J.-H. Chung, D. G. Nocera, and Y. S. Lee, Phys. Rev. Lett. **98**, 107204 (2007).

[2] T.-H. Han, J. S. Helton, S. Chu, D. G. Nocera, J. A. Rodriguez-Rivera, C. Broholm, and Y. S. Lee, Nature (London) **492**, 406 (2012).

[3] C. Zeng and V. Elser, Phys. Rev. B **42**, 8436 (1990).

[4] J. B. Marston and C. Zeng, J. Appl. Phys. **69**, 5962 (1991).

[5] P. Lecheminant, B. Bernu, C. Lhuillier, L. Pierre, and P. Sindzingre, Phys. Rev. B **56**, 2521 (1997).

[6] P. Nikolic and T. Senthil, Phys. Rev. B **68**, 214415 (2003).

[7] R. R. P. Singh and D. A. Huse, Phys. Rev. B **76**, 180407 (2007).

[8] Y. Ran, M. Hermele, P. A. Lee, and X.-G. Wen, Phys. Rev. Lett. **98**, 117205 (2007).

[9] G. Evenbly and G. Vidal, Phys. Rev. Lett. **104**, 187203 (2010).

[10] S. Yan, D. A. Huse, and S. R. White, Science **332**, 1173 (2011).

[11] S. Depenbrock, I. P. McCulloch, and U. Schollwöck, Phys. Rev. Lett. **109**, 067201 (2012).

[12] H.-C. Jiang, Z. Wang, and L. Balents, Nat. Phys. **8**, 902 (2012).

[13] Y. Iqbal, F. Becca, S. Sorella, and D. Poilblanc, Phys. Rev. B **87**, 060405 (2013).

[14] B. K. Clark, J. M. Kinder, E. Neuscamman, G. K.-L. Chan, and M. J. Lawler, Phys. Rev. Lett. **111**, 187205 (2013).

[15] B. Bauer, L. Cincio, B. P. Keller, M. Dolfi, G. Vidal, S. Trebst, and A. W. W. Ludwig, Nat. Commun. **5**, 5137 (2014).

[16] K. Matan, D. Grohol, D. G. Nocera, T. Yildirim, A. B. Harris, S. H. Lee, S. E. Nagler, and Y. S. Lee, Phys. Rev. Lett. **96**, 247201 (2006).

[17] D. A. Huse and A. D. Rutenberg, Phys. Rev. B **45**, 7536 (1992).

[18] C. L. Henley, Phys. Rev. B **80**, 180401 (2009).

[19] K. Hida, J. Phys. Soc. Jpn. **69**, 4003 (2000).

[20] C. Xu and J. E. Moore, Phys. Rev. B **76**, 104427 (2007).

[21] O. Götze, D. J. J. Farnell, R. F. Bishop, P. H. Y. Li, and J. Richter, Phys. Rev. B **84**, 224428 (2011).

[22] A. Läuchli, S. Dommange, B. Normand, and F. Mila, Phys. Rev. B **76**, 144413 (2007).

[23] S. K. Pati and C. N. R. Rao, Chem. Commun. **39**, 4683 (2008).

[24] S. Hara, H. Sato, and Y. Narumi, J. Phys. Soc. Jpn. **81**, 073707 (2012).

[25] D. E. Freedman, R. Chisnell, T. M. McQueen, Y. S. Lee, C. Payen, and D. G. Nocera, Chem. Commun. **48**, 64 (2012).

[26] K. Okuta, S. Hara, H. Sato, Y. Narumi, and K. Kindo, J. Phys. Soc. Jpn. **80**, 063703 (2011).

[27] K. Damle and T. Senthil, Phys. Rev. Lett. **97**, 067202 (2006).

[28] S. V. Isakov and Y. B. Kim, Phys. Rev. B **79**, 094408 (2009).

[29] I. Affleck, T. Kennedy, E. H. Lieb, and H. Tasaki, Phys. Rev. Lett. **59**, 799 (1987).

[30] T. Matsushita, N. Hamaguchi, K. Shimizu, N. Wada, W. Fujita, K. Awaga, A. Yamaguchi, and H. Ishimoto, J. Phys. Soc. Jpn. **79**, 093701 (2010).

[31] K. Hida, J. Phys. Soc. Jpn. **70**, 3673 (2001).

[32] S. R. White, Phys. Rev. Lett. **69**, 2863 (1992).

[33] E. M. Stoudenmire and S. R. White, Annu. Rev. Condens. Matter Phys. **3**, 111 (2012).

[34] D. P. Arovas, Phys. Rev. B **77**, 104404 (2008).

[35] W. Li, S. Yang, M. Cheng, Z.-X. Liu, and H.-H. Tu, Phys. Rev. B **89**, 174411 (2014).

[36] P. Corboz, K. Penc, F. Mila, and A. M. Läuchli, Phys. Rev. B **86**, 041106 (2012).

[37] The energy of the HSS wave function is found to be lower than that reported previously [19].

[38] The reported series expansion estimate of $E_0 = -1.4468$ [19] does not agree with our DMRG result.

[39] Z. Cai, S. Chen, and Y. Wang, J. Phys.: Condens. Matter **21**, 456009 (2009).

[40] P. Zanardi and N. Paunković, Phys. Rev. E **74**, 031123 (2006).

[41] K. Penc and A. M. Läuchli, *Introduction to Frustrated Magnetism*, Springer Series in Solid-State Sciences Vol. 164 (Springer, Berlin, 2011), p. 331.

[42] M. Oshikawa, M. Yamanaka, and I. Affleck, Phys. Rev. Lett. **78**, 1984 (1997).

[43] T. Liu, W. Li, A. Weichselbaum, J. von Delft, and G. Su, Phys. Rev. B **91**, 060403 (2015).

[44] T. Picot and D. Poilblanc, Phys. Rev. B **91**, 064415 (2015).